RADC-TDR-62-473

H-F PROPAGATION SIMULATION

R. Mather
F. Wilson

TECHNICAL DOCUMENTARY REPORT NO. RADC-TDR-62-473

November 1962

Space Defense Systems Laboratory
Rome Air Development Center
Air Force Systems Command
Griffiss Air Force Base, New York

Project No. 5582, Task No. 558203

ABSTRACT

An experiment is described in which high frequency electromagnetic wave propagation is to be simulated on an analog computer and compared with experimental data collected over a 3800-km path. The experimental complex consists of a transmitter site located in the Panama Canal Zone and a receiver site at Stockbridge, NY. Vertical ionospheric sounders are located along the transmission path and are used to measure the spatial distribution of electron density in the volume of interest. A method is described whereby this spatial distribution of electron density is programmed into the analog computer in order that the Hamiltonian equations describing ray paths may be solved. In addition to producing frequency vs. time plots for comparison with the experimental data, the simulator also gives results not easily measured in the field, such as take-off angle, angle of arrival, group time, phase time, off-path deviation, and height of reflection.

An alternate use for the simulator is also presented. By rescaling the problem and making use of its capability to generate functions of three variables, one can examine the effects of small-scale irregularities of ionization on electromagnetic waves.

PUBLICATION REVIEW

This report has been reviewed and is approved.

Approved: Joseph Fallik
JOSEPH FALLIK
Chief, Space Defense Systems Laboratory
Directorate of Aerospace
Surveillance & Control

Approved: William B. Bryant
JAMES B. BRYANT
Colonel, USAF
Director of Aerospace
Surveillance & Control

FOR THE COMMANDER: Irving J. Gabelman
IRVING J. GABELMAN
Director of Advanced Studies

AIR FORCE, Cato Show Prtg. Co. 11/20/62 - 172

TABLE OF CONTENTS

LIST OF ILLUSTRATIONS

H-F PROPAGATION SIMULATION*

A. INTRODUCTION

Ever since the discovery of the multilayer ionosphere by Appleton[1] in 1925 and the subsequent development of the echo sounding technique by Breit and Tuve[2] in 1926, man has made constant and ever-increasing use thereof as a refractory medium for over-the-horizon propagation of electromagnetic waves. Since the make-up and behavior of the ionosphere is complex, it refracts and returns electromagnetic waves in a very complicated manner. Knowledge of the ionosphere came about gradually and as this knowledge grew, the usefulness and utilization also increased. As utilization increases, our desire and need for still more detailed knowledge also increase. Each application of new knowledge opens new horizons, and poses additional problems to solve and more questions to answer. Approximations once valid may no longer be appropriate in newer applications.

B. ECHO SOUNDING TECHNIQUES

1. Vertical Sounders

Many practical aids, both passive and active, have been developed to help communication engineers select optimum circuit parameters for reliable transmission between specified locations. The "echo sounding technique" or vertical sounder of Breit and Tuve, and variations thereof, is still the most widely used tool for ionospheric research and ionospheric morphology studies. With this device a succession of pulses stepped in frequency (usually from 1 to 25 mc) are transmitted at vertical incidence to the ionosphere and received at measured time delays. Since the electron density required for complete refraction of a normally incident electromagnetic wave is a known function of frequency, an electron density vs. height profile can be obtained in a radarlike fashion. However, since the ionosphere is dispersive, the group and phase velocity vary considerably over the path. Free-space propagation velocity must necessarily be assumed, and the heights thus obtained are "virtual" rather than true.

Methods have been devised to convert these virtual height records into true height profiles[3,4]. An inherent weakness in this sounding method is that returns can be obtained only where the electron density is increasing monotonically with height. When this condition does not exist, as immediately above each intermediate layer and above the peak of the topmost (F_2) layer, gaps result in the data. A vertical sounding record along with the resultant true height profile is shown in Figure 1.

Hundreds of these vertical sounders located all over the world provide voluminous amounts of statistical data on the behavior of the ionosphere (temporal, seasonal, sun spot angle, etc.). From these data the National Bureau of Standards compiles and publishes "Basic Radio Propagation Predictions" which are monthly contour charts of predicted ionospheric parameters. These monthly predictions are supplemented by a weekly

* Released 1 October 1962.

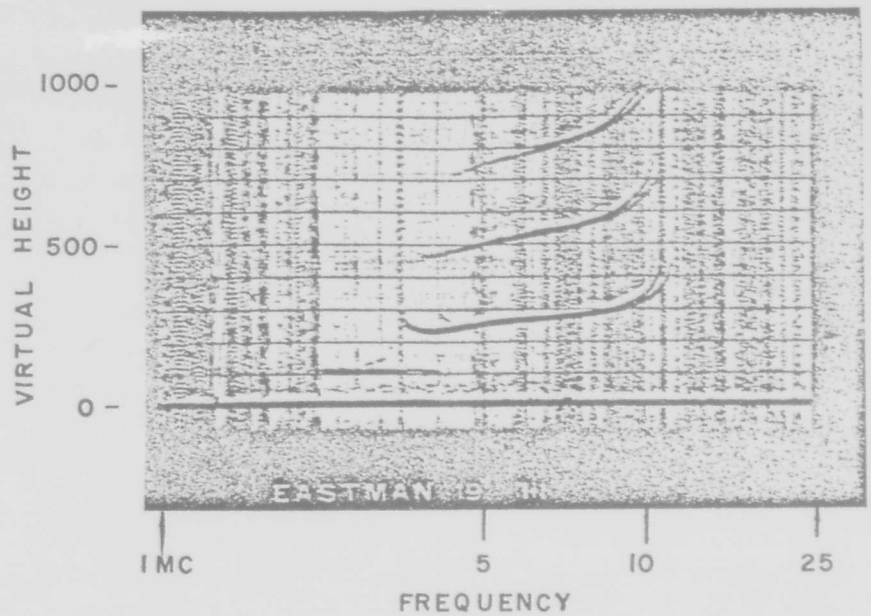

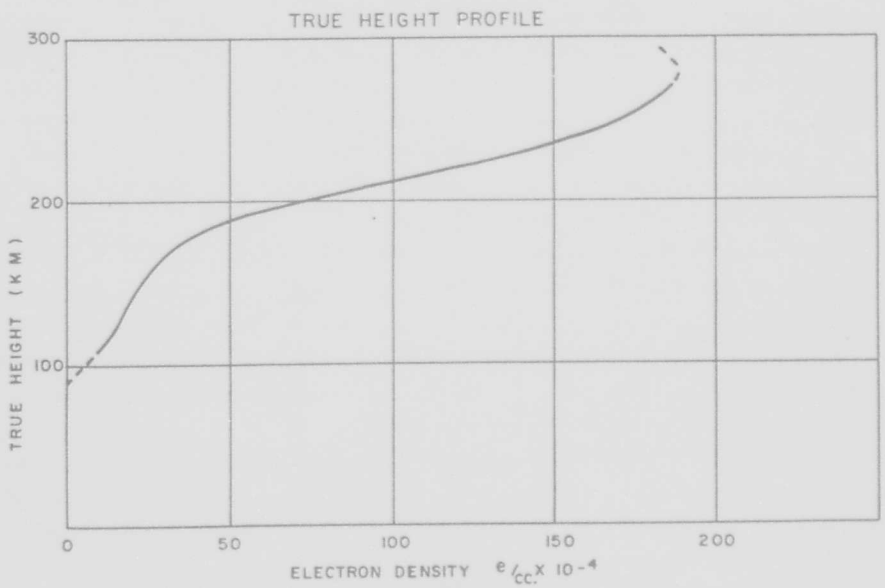

Figure 1. Puerto Rico Vertical Sweep Frequency Sound.

(published) and hourly (WWV broadcast) warning service for unusual and disturbed conditions. Experienced communicators make effective use of these predictions in choosing operating frequencies for point-to-point communications.

2. Backscatter Sounders

There are also active techniques available whenever real time information on point-to-point propagation conditions is desired. One such technique is the backscatter sounder, which is a modification of the vertical sounder. Instead of transmitting vertically, and receiving energy directly from the ionosphere, the energy is directed obliquely over some desired propagation path. The received energy in this case is ground backscatter, returned from beyond line-of-sight via ionospheric refraction. The display is frequency vs. range (see Figure 2). From a real time readout of this device, an operator can determine the frequency best suited to illuminate the zone of interest.

3. Oblique Sounders

A still further extension of the sounding techniques are the oblique sounders. In this case the transmitter and synchronous receiver are at opposite ends of a propagation link. The received display is frequency vs. time (Figure 3). The *major* modes can be separated and identified at discrete frequencies by experienced operators. This information, together with past experience, i.e., what the hourly trends are likely to be, help the operator select optimum frequencies for communication over *that particular* circuit.

C. H-F RESEARCH

These useful devices all play a very important role in H-F communications and ionospheric research. However, none of them yield much information about the path over which the energy travels from the transmitter to the receiver. Indeed, the received energy is usually a superposition of many signals from a single origin, but arriving over many different ray paths, and thus having different transit times. While it is true that the oblique sounder separates the *major* modes over *one* particular circuit, it does not yield information about the asymmetry of the ray paths. Experiments using direction-finding equipment have shown that, in general, most of the received energy arrives at the receiver at some angle off the great circle path. This is due to the influence of the horizontal gradients of electron density in the azimuthal plane and the effects of the earth's magnetic field.

Recently, interest has been shown in the possibility of developing over-the-horizon radars at high frequency. If this is to be a fruitful endeavor, then inevitably these second-order effects must be studied in greater detail. Coverage may be more critical and will most likely be in terms of volumes of space rather than zones on the earth. Accuracy will depend upon detailed knowledge of the asymmetry of the ray paths. Resolution will depend upon the ability to separate and identify ray paths. New and unique methods of "sounding" the ionosphere in order to determine the fine grain spatial distribution of electron density will be desirable, if not an absolute necessity.

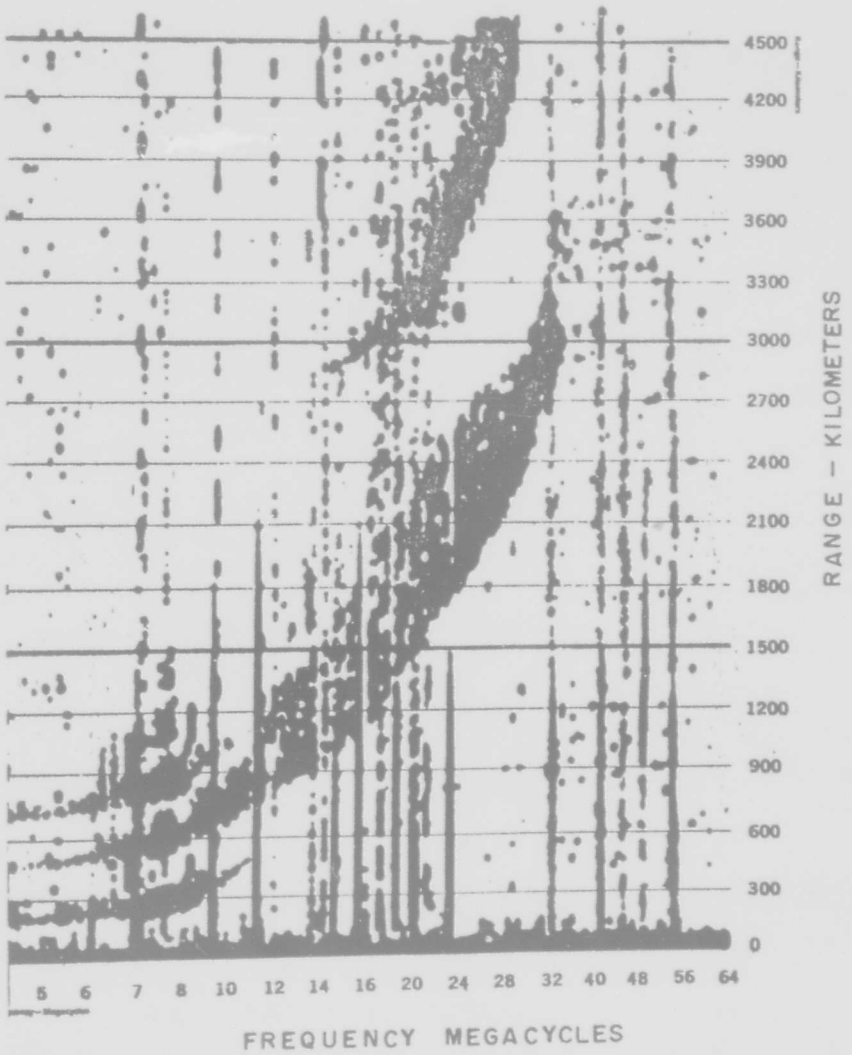

Figure 2. Typical Backscatter Sounding Record.

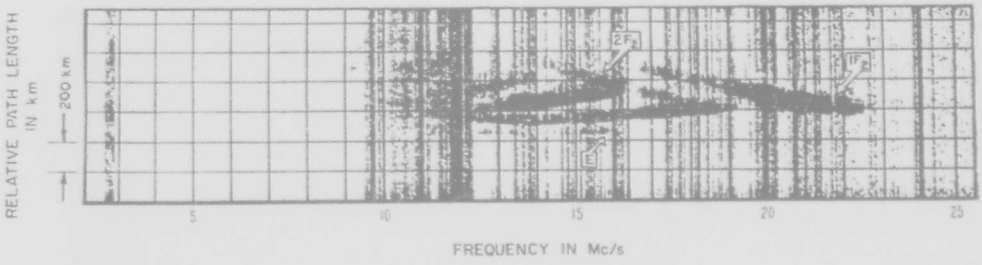

Figure 3. Typical Oblique Incidence Ionogram.

D. PROPAGATION EFFECTS STUDY

1. An Experimental Program

In the experiment described here, we attempt to simulate and study these second-order propagation effects. A block diagram of the experiment is shown in Figure 4. A tunable short-pulse transmitter is located at Panama along with an oblique sounder transmitter. Also in the Panama area is a vertical incident ionospheric sounder. The short-pulse receiver and oblique sounder receiver are located at Stockbridge, N.Y. At least four additional sounders are located along the great circle path between the transmitter and receiver. The co-ordinate system used is shown in Figure 5. The short (10 μsec) pulse equipment is used to separate paths not resolvable with the relatively long pulse step frequency sounders. The frequency selection for the short pulse transmitter will be based on the real time readout of the oblique sounder. The vertical sounders located along the path provide the necessary sounding data during the times of interest. The raw data from the vertical sounders will be reduced to true height profiles $N(h)$ and $\frac{\partial N}{\partial h}$. With this having been done, the data will be in the proper form for direct input into the propagation simulator.

The most unique part of the experiment is the propagation simulator or analog computer. The straightforward, though ambitious, manner in which the analog computer is used to simulate H-F propagation is as follows.

2. Mathematical Derivation

The Hamiltonian equations as derived by Haselgrove[5] describing ray paths in a general three-dimensional magneto-ionic medium using an earth-centered spherical co-ordinate system (r, θ, ϕ) are:

$$\frac{dr}{dt} = \frac{1}{\mu^2}\left[\rho_r - \mu\frac{\partial\mu}{\partial\rho_r}\right] \tag{1}$$

$$\frac{d\theta}{dt} = \frac{1}{r\mu^2}\left[\rho_\theta - \mu\frac{\partial\mu}{\partial\rho_\theta}\right] \tag{2}$$

$$\frac{d\phi}{dt} = \frac{1}{r\mu^2\sin\theta}\left[\rho_\phi - \mu\frac{\partial\mu}{\partial\rho_\phi}\right] \tag{3}$$

$$\frac{d\rho_r}{dt} = \frac{1}{\mu}\frac{\partial\mu}{\partial r} + \rho_\theta\frac{d\theta}{dt} + \rho_\phi\sin\theta\frac{d\phi}{dt} \tag{4}$$

$$\frac{d\rho_\theta}{dt} = \frac{1}{r}\left[\frac{1}{\mu}\frac{\partial\mu}{\partial\theta} - \rho_\theta\frac{dr}{dt} + r\rho_\phi\cos\theta\frac{d\phi}{dt}\right] \tag{5}$$

$$\frac{d\rho_\phi}{dt} = \frac{1}{r\sin\theta}\left[\frac{1}{\mu}\frac{\partial\mu}{\partial\phi} - \rho_\phi\sin\theta\frac{dr}{dt} - r\rho_\phi\cos\theta\frac{d\theta}{dt}\right] \tag{6}$$

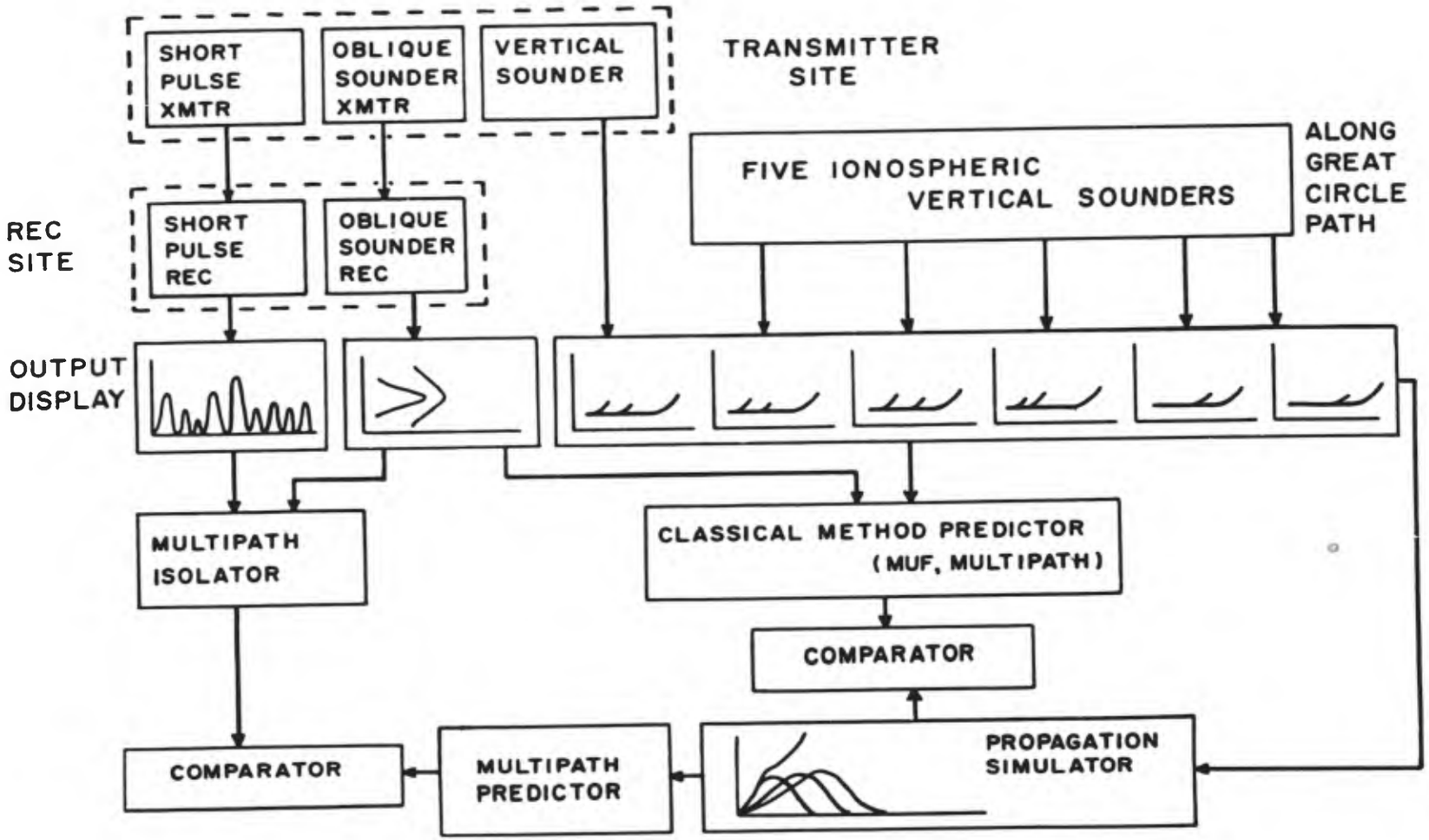

Figure 4. Proposed H-F Experimental Program.

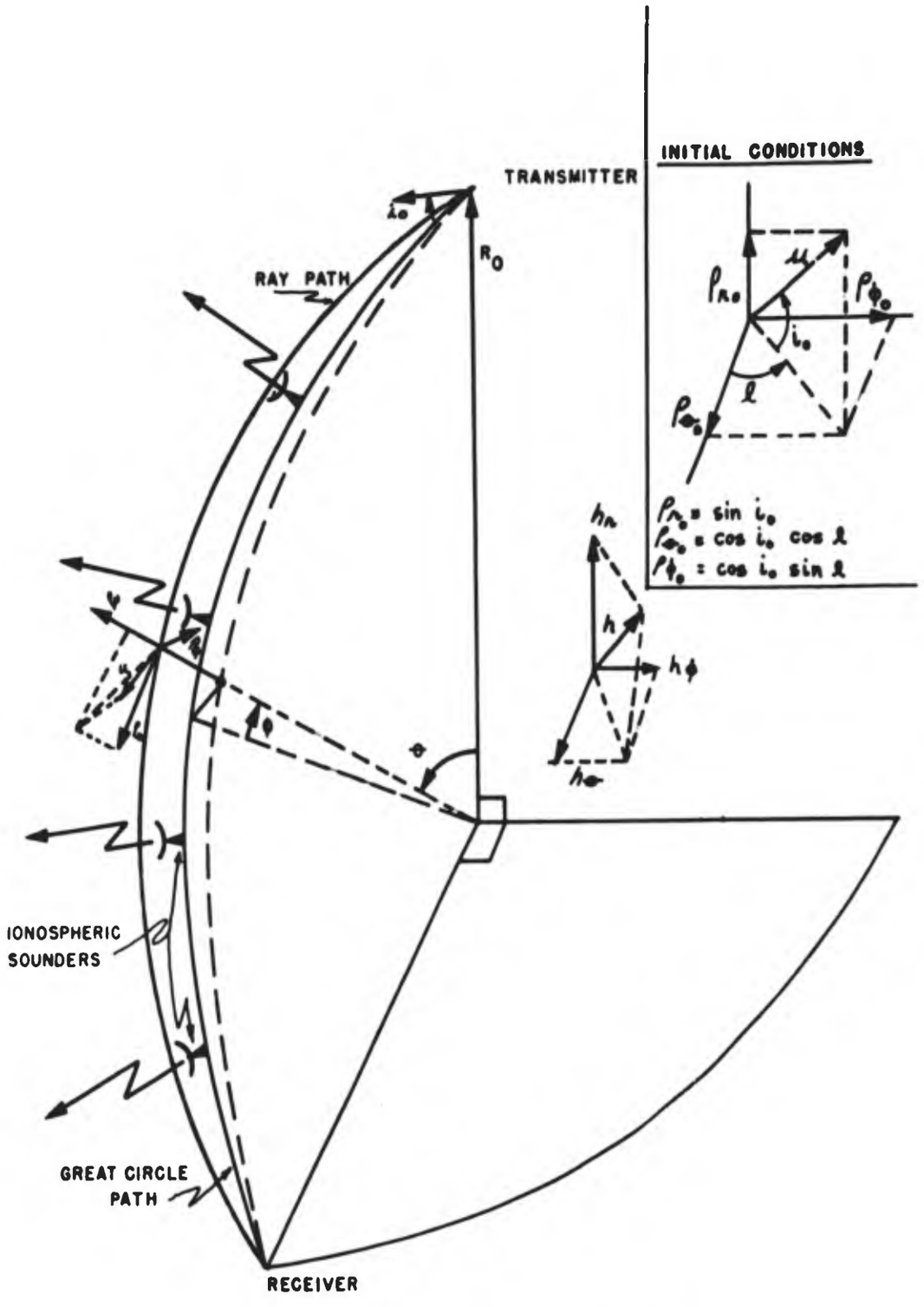

Figure 5. General Co-ordinate System.

The paths that the rays propagate, as determined by these equations, are dependent on the spatial distribution of the index of refraction which is a function of the frequency of transmission, the orientation and magnitude of the earth's magnetic field, and the spatial distribution of electron density $N(r, \theta, \phi)$. This index of refraction, μ, is given by the Appleton-Hartree formula for negiigible collisions:

$$\mu^2 = 1 - \frac{2a(1-a)}{2(1-a) - h\sin^2 a \pm \sqrt{h^2 \sin^4 a + 4h(1-a)^2 \cos^2 a}} \tag{7}$$

It may be demonstrated[6] that for practical cases of interest and for operating frequencies above 10 mc, the formula for μ may be reduced to:

$$\mu^2 = 1 - \frac{a}{1 \pm C^{\frac{1}{2}} \cos a} \tag{8}$$

with a sacrifice of only 2% in precision. From (8) the necessary derivatives are formed and substituted into the original Haselgrove equations as follows:

$$\frac{dr}{dt} = \frac{1}{\mu^2}\left[\rho_r \pm \frac{FF_h}{81}\frac{1}{N}\frac{h_r}{h}\frac{(1-\mu^2)^2}{2\mu} \pm \frac{\rho_r F^2}{81N}\frac{(1-\mu^2)}{2\mu^2}\left(1-\mu^2-\frac{81N}{F^2}\right)\right] \tag{9}$$

$$\frac{d\theta}{dt} = \frac{1}{r\mu^2}\left[\rho_\theta \pm \frac{FF_h}{81}\frac{1}{N}\frac{h_\theta}{h}\frac{(1-\mu^2)^2}{2\mu} \pm \frac{\rho_\theta F^2}{81N}\frac{(1-\mu^2)}{2\mu^2}\left(1-\mu^2-\frac{81N}{F^2}\right)\right] \tag{10}$$

$$\frac{d\phi}{dt} = \frac{1}{r\mu^2\sin\theta}\left[\rho_\phi \pm \frac{FF_h}{81}\frac{1}{N}\frac{h_\phi}{h}\frac{(1-\mu^2)^2}{2\mu} \pm \frac{\rho_\phi F^2}{81N}\frac{(1-\mu^2)}{2\mu^2}\left(1-\mu^2-\frac{81N}{F^2}\right)\right] \tag{11}$$

$$\frac{d\rho_r}{dt} = -\frac{(1-\mu^2)}{2\mu^2}\frac{1}{N}\frac{\partial N}{\partial r} + \rho_\theta\frac{d\theta}{dt} + \rho_\phi\frac{d\phi}{dt}\sin\theta \tag{12}$$

$$\frac{d\rho_\theta}{dt} = \frac{1}{r}\left[-\frac{(1-\mu^2)}{2\mu^2}\frac{1}{N}\frac{\partial N}{\partial\theta} - \rho_\theta\frac{dr}{dt} + r\rho_\phi\cos\theta\frac{d\phi}{dt}\right] \tag{13}$$

$$\frac{d\rho_\phi}{dt} = \frac{1}{r\sin\theta}\left[-\frac{(1-\mu^2)}{2\mu^2}\frac{1}{N}\frac{\partial N}{\partial\phi} - \rho_\phi\sin\theta\frac{dr}{dt} - r\rho_\phi\cos\theta\frac{d\theta}{dt}\right] \tag{14}$$

Since we are dealing with earth radii units and since r is always small compared to R_0, the following change of variables is noted.

$$r = 1 + z$$
$$dr = dz$$

With the above substitution the equations become:

$$\frac{dz}{dt} = \frac{1}{\mu^2}\rho_r \pm \frac{1}{2\mu^3}\frac{FF_h}{81}\frac{1}{N}\frac{h_r}{h}(1-\mu^2)^2 \pm \frac{\rho_r F^2}{81N}\frac{(1-\mu^2)}{2\mu^4}\left(1-\mu^2-\frac{81N}{F^2}\right) \quad (15)$$

$$(1+z)\frac{d\theta}{dt} = \frac{1}{\mu^2}\rho_\theta \pm \frac{(1-\mu^2)^2}{2\mu^3}\frac{FF_h}{81}\frac{1}{N}\frac{h_\theta}{h} \pm \frac{\rho_\theta F^2}{81N}\frac{(1-\mu^2)}{2\mu^4}\left(1-\mu^2-\frac{81N}{F^2}\right) \quad (16)$$

$$\sin\theta(1+z)\frac{d\phi}{dt} = \frac{1}{\mu^2}\rho_\phi \pm \frac{1}{2\mu^3}\frac{FF_h}{81}\frac{1}{N}\frac{h_\phi}{h}(1-\mu^2)^2 \pm \frac{\rho_\phi F^2}{81N}\frac{(1-\mu^2)}{2\mu^4}$$

$$\left(1-\mu^2-\frac{81N}{F^2}\right) \quad (17)$$

$$\frac{d\rho_r}{dt} = \rho_\theta\frac{d\theta}{dt} + \rho_\phi \sin\theta\frac{d\phi}{dt} - \frac{(1-\mu^2)}{2\mu^2}\frac{1}{N}\frac{\partial N}{\partial z} \quad (18)$$

$$(1+z)\frac{d\rho_\theta}{dt} = (1+z)\rho_\phi\cos\theta\frac{d\phi}{dt} - \rho_\theta\frac{dz}{dt} - \frac{(1-\mu^2)}{2\mu^2}\frac{1}{N}\frac{\partial N}{\partial\theta} \quad (19)$$

$$\sin\theta(1+z)\frac{d\rho_\phi}{dt} = -(1+z)\rho_\phi\cos\theta\frac{d\theta}{dt} - \rho_\phi\sin\theta\frac{dz}{dt} - \frac{(1-\mu^2)}{2\mu^2}\frac{1}{N}\frac{\partial N}{\partial\phi}. \quad (20)$$

The above equations were appropriately scaled in time and amplitude in accordance with the limitations of the computer. The resultant time for an average one-hop 3000-KM trace is about 45 seconds. This time scaling was a best compromise between interpolation errors experienced in long computer runs and the servo multiplier errors that occur at higher speeds.

In addition to the ray paths, it is necessary to compute the group time of travel T from transmitter to receiver. The following equation applies:

$$\frac{dT}{dt} = \frac{1}{c}\left(1+\frac{F}{\mu}\frac{\partial\mu}{\partial F}\right)$$

Since

$$\frac{\partial\mu}{\partial F} = \frac{a}{\mu F\left(1 \pm G^{1/2}\cos a\right)}$$

then

$$\frac{dT}{dt} = \frac{1}{c\mu^2}$$

The initial conditions are:

$$\rho_{r_0} = \sin i_0$$

$$\rho_{\theta_0} = \cos i_0 \cos l$$

$$\rho_{\phi_0} = \cos i_0 \sin l.$$

θ_0 = latitude of starting point.

As may be noted by equations 15-20, the independent variables required for precise ray path simulation are:

$$\frac{hr}{h}, \frac{h\theta}{h}, \frac{h\phi}{h}, N, \frac{\partial N}{\partial z}, \frac{\partial N}{\partial \theta}, \frac{\partial N}{\partial \phi}.$$

These terms are all nonlinear functions of z, θ, ϕ. The variables $\frac{hr}{h}, \frac{h\theta}{h}, \frac{h\phi}{h}$ which describe the earth's magnetic field are relatively easy to handle. They are well known quantities along the path of interest and do not change appreciably with the height or off-path excursions we expect to experience. See Figure 6. Once having been "read in" to the computer these functions remain the same for all ray tracings along this path. It was therefore deemed expedient to use the less flexible but also less expensive servo pot padding technique for generating these functions.

3. Representation of Electron Density Distribution

The kernel of the problem lies in the remaining four independent variables, i.e., the spatial distribution of electron density. Close examination of equations 15-20 shows that the major refractory effects on the wave normal vector are determined by these terms. To attempt to construct a device capable of generating each of these terms precisely as an independent function of z, θ, ϕ would be formidable. However, no device exists today which can measure these quantities over any appreciable spatial volume. Therefore, it seemed more realistic to design our analog function generating equipment with capabilities of the same order as our measuring devices, but, at the same time, flexible to insure the possibility of future improvements.

The method used is as follows: We have five sounders available along the agent circle path (Figure 5). Each sounder provides $(\frac{\partial N}{\partial z})$ for discrete values of θ and for $\phi = 0$. These five partials are "read" into diode function generators (dfg's). Figure 7 shows five partials for discrete values of θ. Linear interpolation is made by proper use of servos for intermediate values of θ along the path. The output of the servo is now $(\frac{\partial N}{\partial z})$ as a function of θ. $\frac{\partial N}{\partial \theta}$ must be similarly obtained. First N vs. θ is plotted for five judiciously chosen heights along the path. $\frac{\partial N}{\partial \theta}$ is then calculated for each of these heights and read into diode function generators (Figure 8). With servo interpolation we have $\frac{\partial N}{\partial \theta}$ as a function of z. Figure 9c shows the computer's flow diagram for the formation of $\frac{\partial N}{\partial z}$ and $\frac{\partial N}{\partial \theta}$.

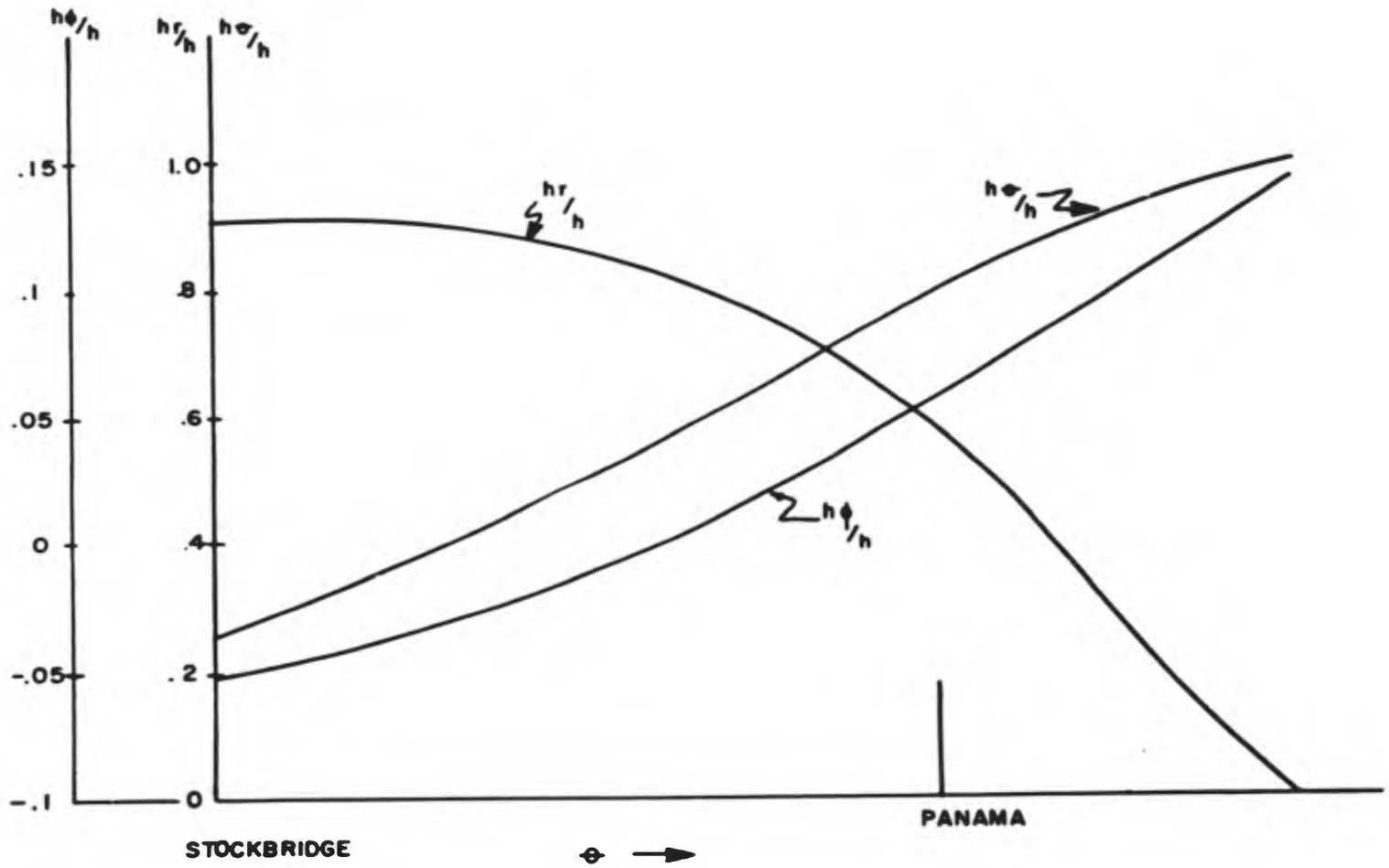

Figure 6. Earth's Magnetic Field Variables as Functions of θ.

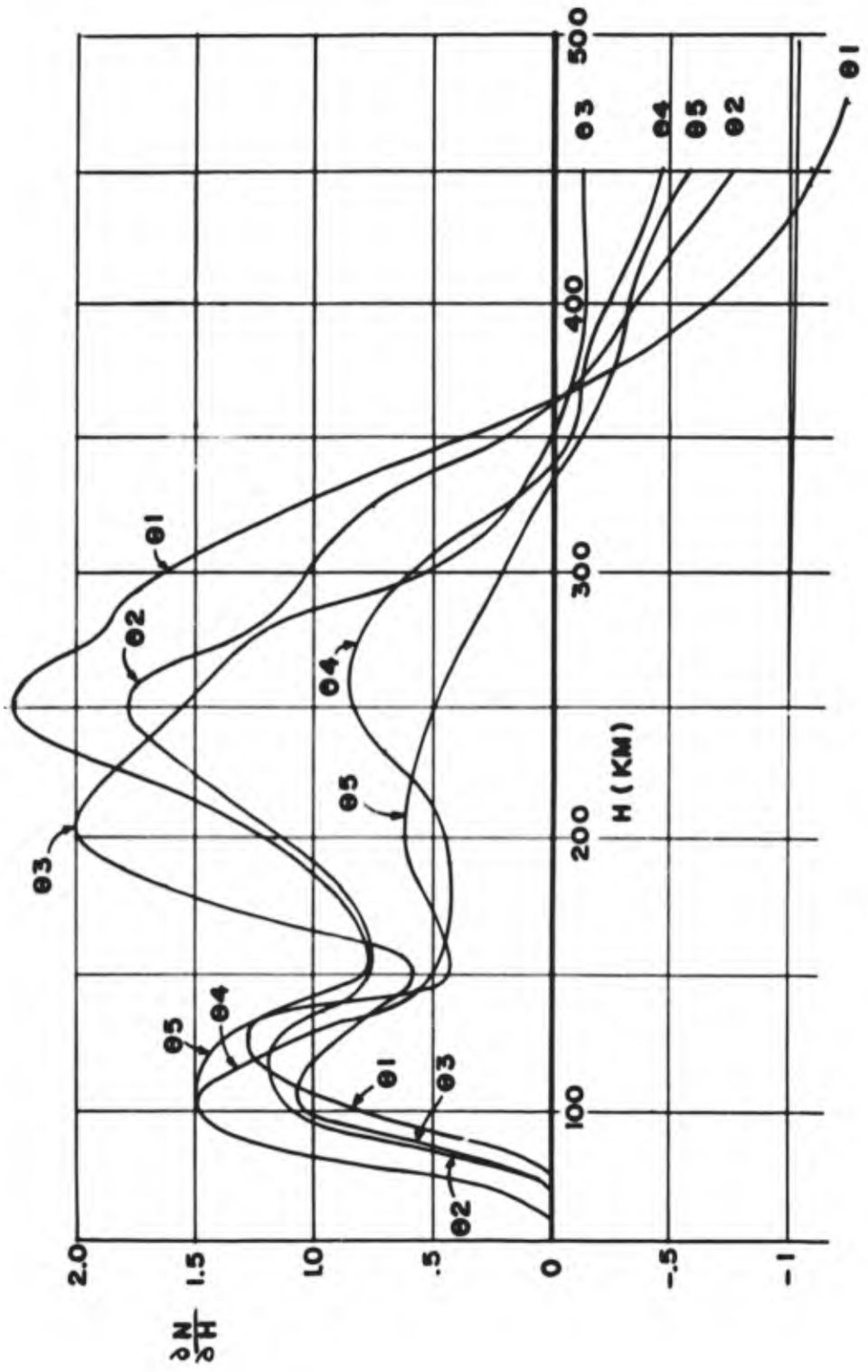

Figure 7. $\frac{\partial N}{\partial H}$ versus H.

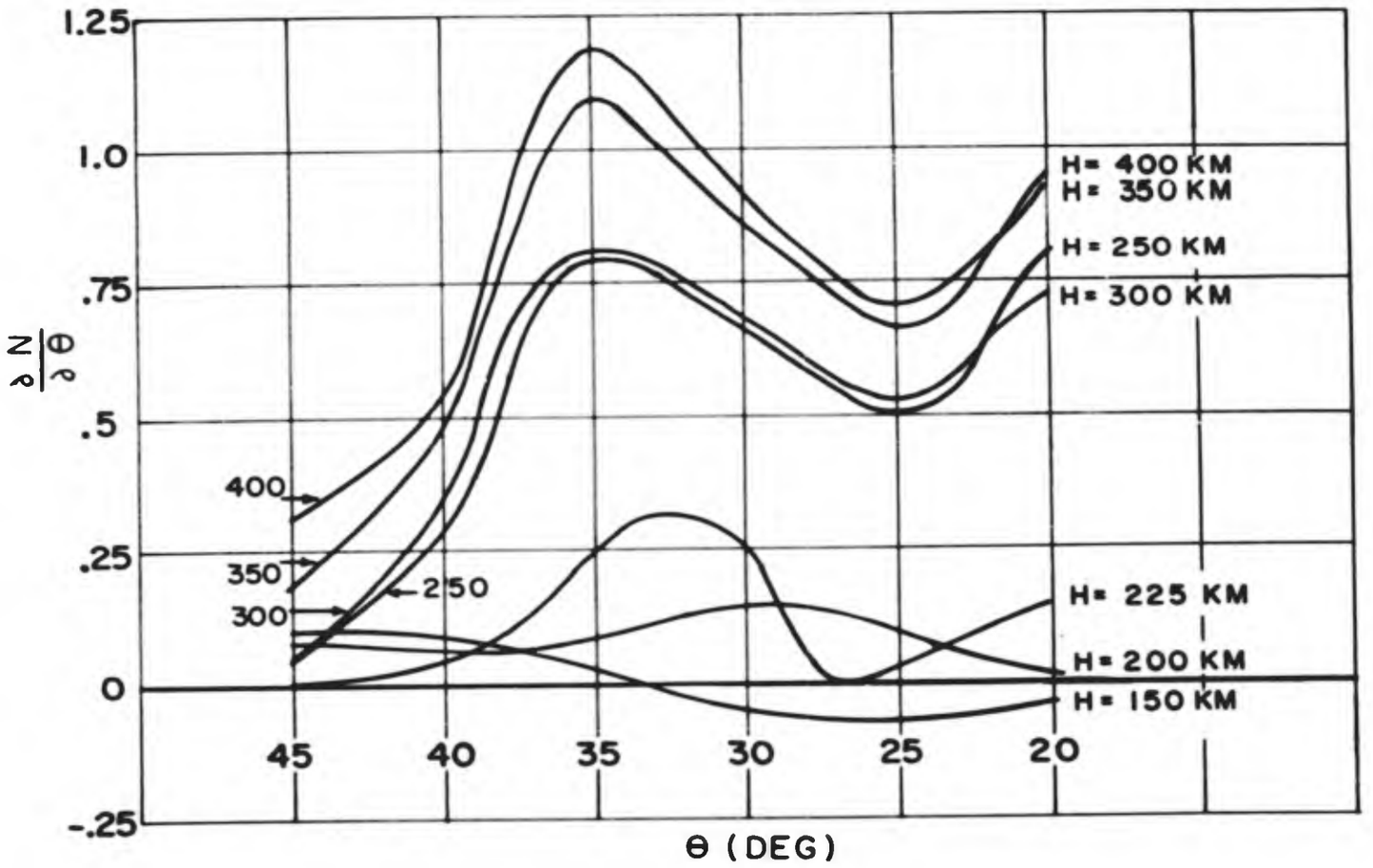

Figure 8. $\frac{\partial N}{\partial \theta}$ versus θ.

It would seem logical to form $\frac{\partial N}{\partial \phi}$ in a similar manner (i.e., combinations of diode function generators and servo). However, we do not have vertical sounders appropriately located in the $\pm \phi$ directions to give lateral distribution of electron density. If they were available it would still be an impractical method because of the unrealistic amounts of diode function generators and servos required. The following alternate approach was taken to represent electron density gradients in the ϕ planes.

Past experience has shown that, since the ionosphere is sun-controlled, there will be a positive or negative gradient in the electron density distribution in the east-west (ϕ) direction, depending on whether the sun is rising or setting. We assume that, for the small lateral distances with which we are concerned, the earth turns under a fixed ionosphere. Based on this assumption, sounder records at $t_0 \pm 20$ min will approximate actual sounders at $\phi = \pm 5°$. From these "before" and "after" samples we determine a linear approximation for the gradient in the lateral direction. The formation of the $\frac{\partial N}{\partial \phi}$ term is taken care of by a single pot.

The spatial distribution of N is also a required quantity and could be obtained in the same manner that the partials of N were obtained. However, this would double the requirement for diode function generators and servos and approximately double the problem set-up time. It is therefore noted that:

$$N = N(z, \theta, \phi)$$

$$\frac{dN}{dt} = \frac{\partial N}{\partial z}\frac{dz}{dt} + \frac{\partial N}{\partial \theta}\frac{d\theta}{dt} + \frac{\partial N}{\partial \phi}\frac{d\phi}{dt}$$

Since all of the quantities on the right are available, N can be obtained by three multipliers and one integrator, a considerable savings in time and equipment.

A flow diagram of the computer program is shown in Figure 9a, b, c. Initial conditions and frequency of operation is taken care of by pot settings. Each set of initial conditions results in two rays, the ordinary and the extra-ordinary. This ray splitting is an effect caused by the earth's magnetic field. Which ray is traced (ordinary or extra-ordinary) depends on the root used in $\pm G^{\frac{1}{2}} \cos \alpha$ (equation 8). This choice is made available on the simulation by a function switch.

4. Comparison of Results

Using the group time versus ground distance outputs of the simulator, A-scope presentations can be constructed to be compared with those from the short pulse receiver. In a like manner, by simulating a sampling of frequencies across the H-F spectrum, oblique sounding records can be constructed. If the simulated records match the actual data, one can demonstrate with some confidence the path each ray traveled from the transmitter to the receiver. We will also be able to produce records along with ray path structure for hypothetical sites within our experimental complex. Attempts will be made to simulate ray paths for a wide variety of ionospheric conditions, i.e., daytime, nighttime, quiet and disturbed ionosphere.

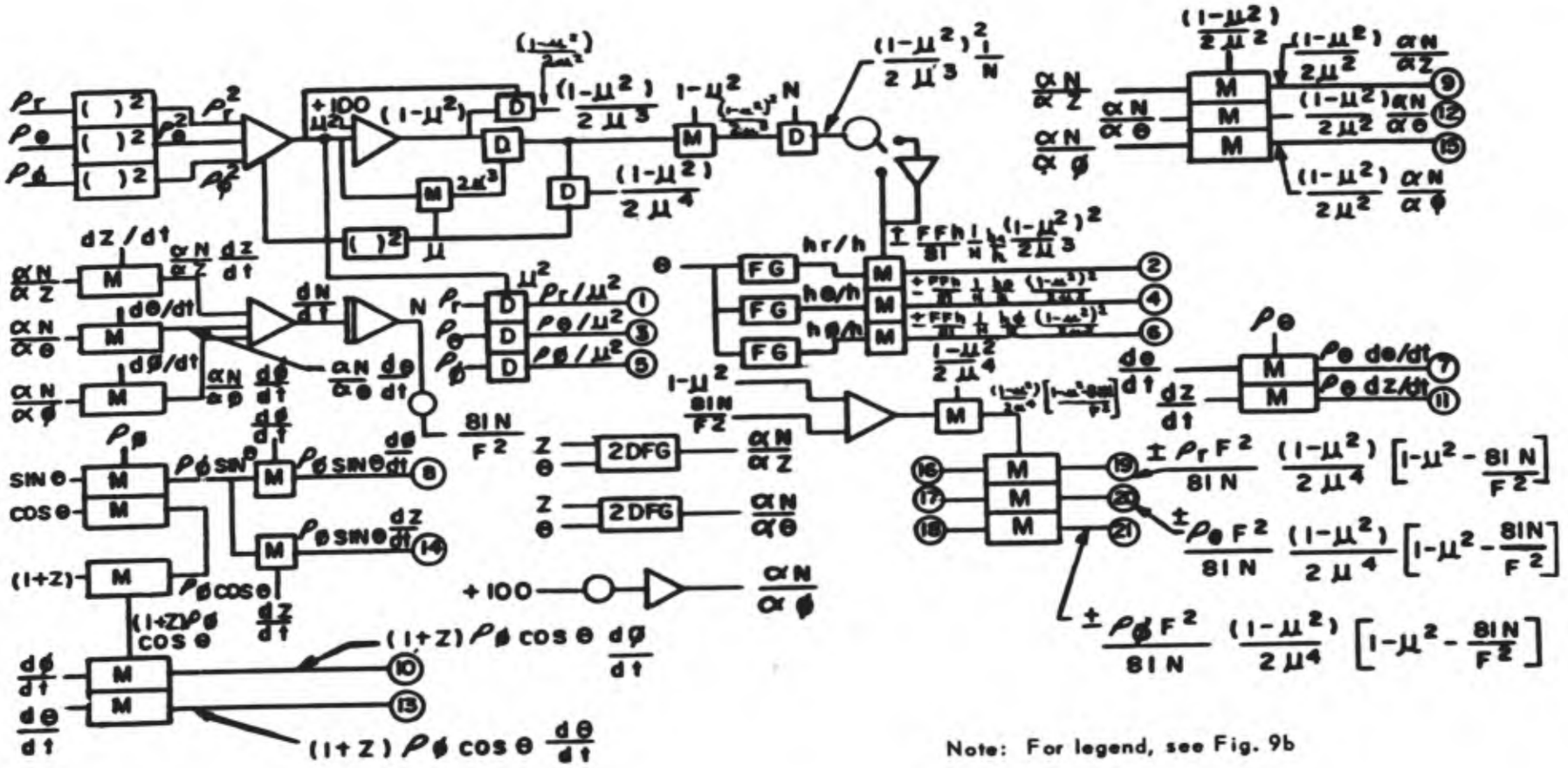

Figure 9a. Basic Computer Diagram.

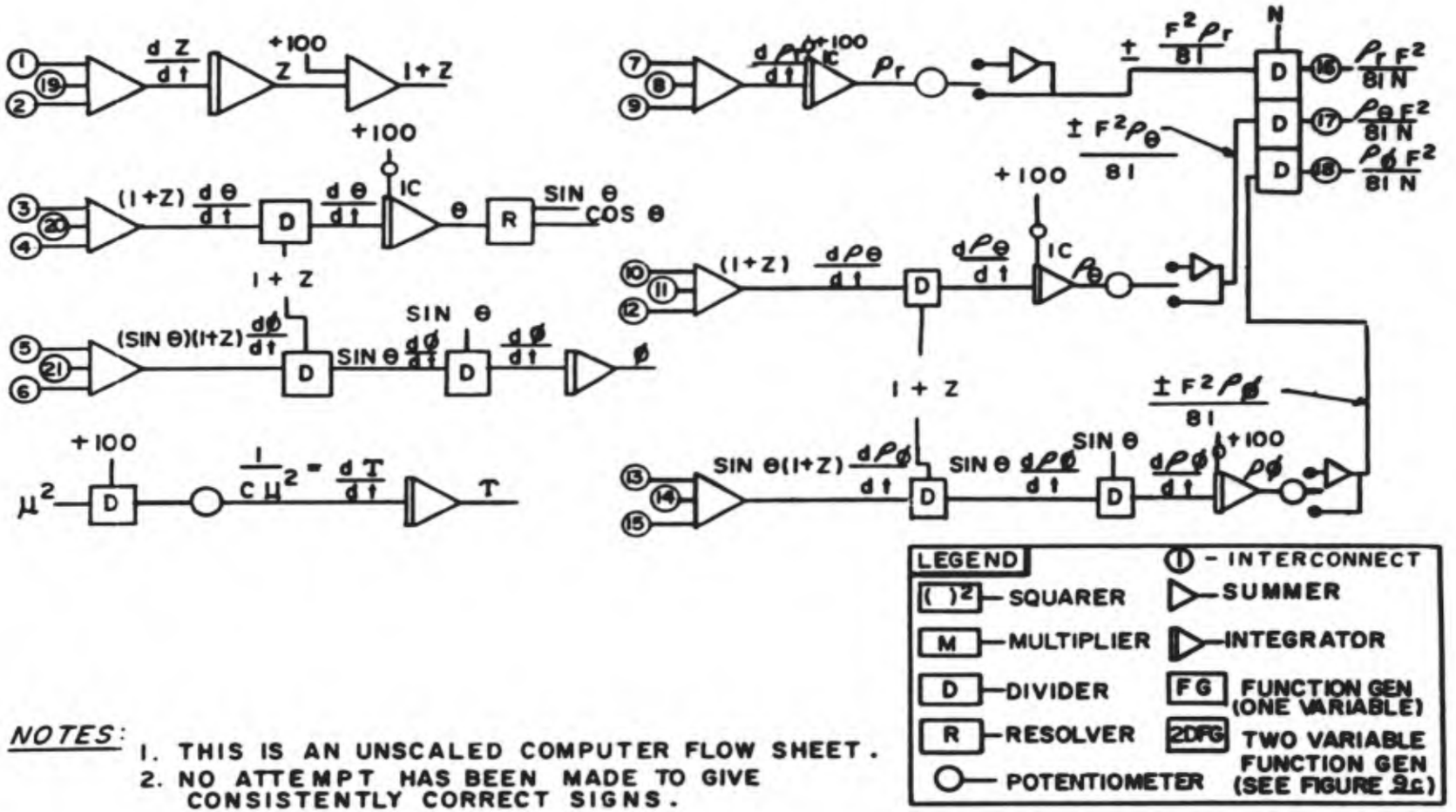

NOTES:
1. THIS IS AN UNSCALED COMPUTER FLOW SHEET.
2. NO ATTEMPT HAS BEEN MADE TO GIVE CONSISTENTLY CORRECT SIGNS.

Figure 9b. Basic Computer Diagram.

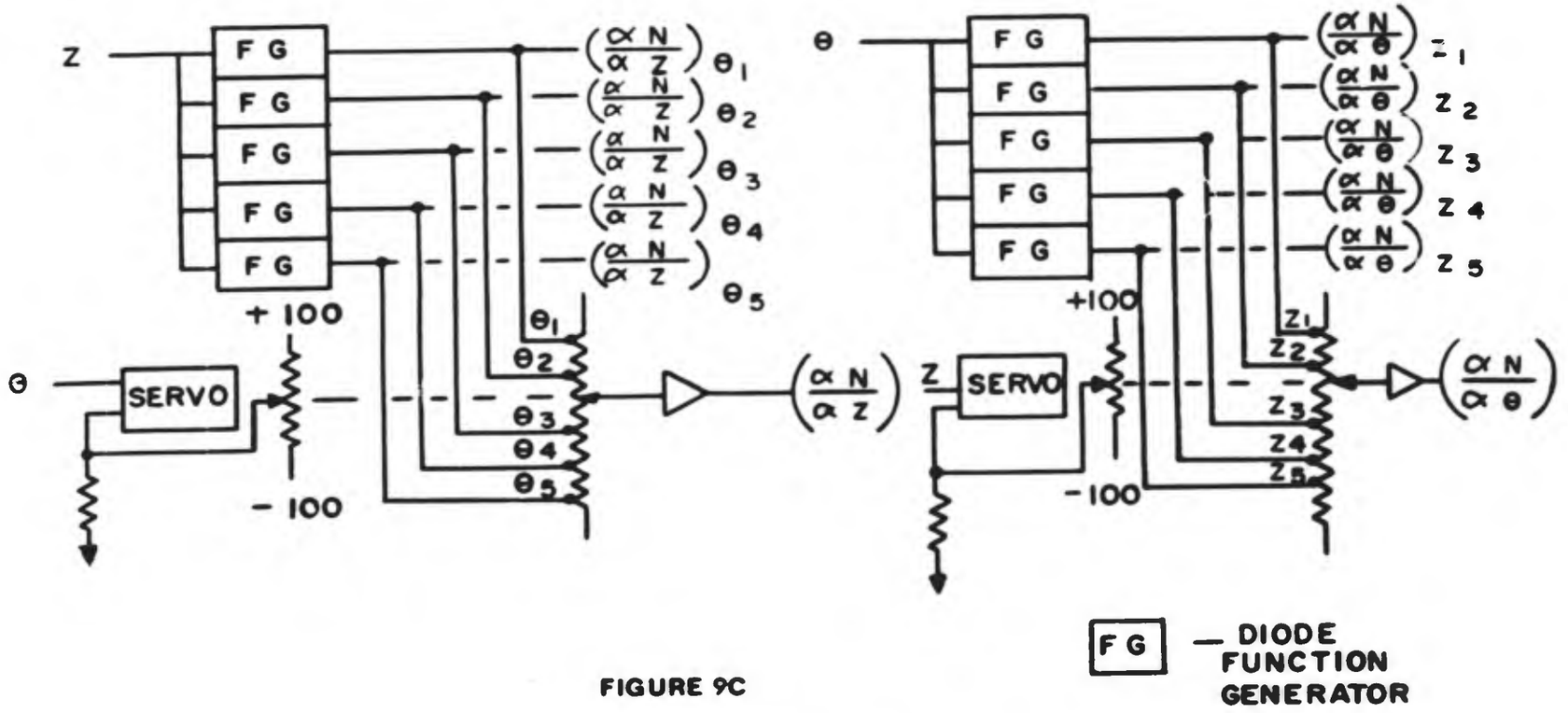

FIGURE 9C

Figure 9c. The Formation of $\frac{aN}{az}$ and $\frac{aN}{a\theta}$ as Functions of z and θ.

E. AN IONIZATION MODEL

The H-F propagation simulator described has the capability of representing the spatial distribution of electron density in two dimensions in terms of five vertical and five horizontal cuts with linear interpolation between cuts. The third or lateral dimension is represented by a linear approximation for the gradient of electron density. If one wished to examine closely the effects of irregularities whose dimensions are small compared with our sampling distance, without the expense of more analog equipment, one could do so by rescaling the problem to smaller volumes. Since there has been speculation about the effects of those small-scale perturbations a sample problem has been worked out for a hypothetical model. It is a cylinder of electron density varying nonlinearly with the radius but varying in a linear fashion along its axis (Figure 10a). The variation of electron density (N) with height for four specific values of ϕ is plotted in Figure 10b. The same curves in Figure 9b apply for N variations with ϕ for specific values of height. The appropriate derivatives $(\frac{\partial N}{\partial z})_{1,2,3,4}$ $(\frac{\partial N}{\partial \phi})_{1,2,3,4}$ are plotted in Figure 10c. Since this model is symmetrical, profiles are not required beyond the axis. An equivalent of a seven by seven matrix is obtained by appropriate use of servos. The electron density along the axis of this model can be made to vary linearly by using one pot and one amplifier or in a nonlinear fashion with a servo multiplier. The effects of a model such as this on a H-F wave can be examined by varying the angle and the frequency of impinging rays.

F. CONCLUSIONS

Every consideration has been given toward making this experiment as flexible as possible. Vertical sounders can be added to or removed from the complex if such a change is indicated by results. However, it would be unrealistic to expect to be able to successfully simulate actual data at all times or under all types of propagation conditions. We have, in a similar experiment and under ideal conditions, been able to simulate actual records with a single vertical sounder at midpath. On the other hand, we feel certain that there are times when propagation simulation would be impossible, even with an unlimited amount of sounders and analog equipment. We can expect valid results only when the electron distribution does not change appreciably in a nonlinear fashion between soundings. Therefore, we believe that the degree of success (or failure) along with the knowledge and experience gained by this experiment will be of use to future designers of over-the-horizon radar systems.

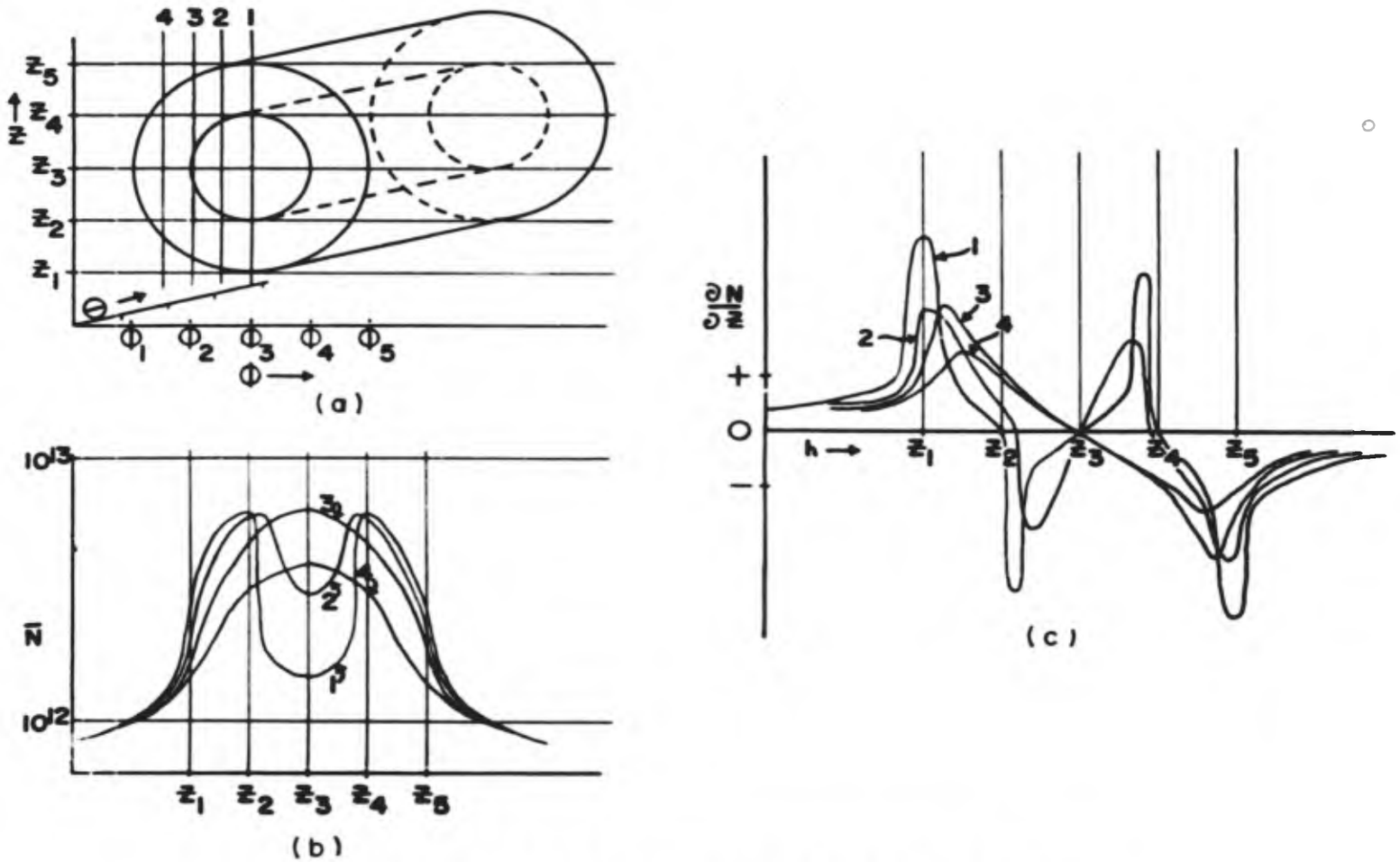

Figure 10. Ionization Model Representation by Diode Function Generators.

BIBLIOGRAPHY

1. Appleton, E.V. and Burnett, M.A.F., *Nature* 115 (1925), 333.
2. Breit, G. and Tuve, *Phys. Rev.* 28 (1926), 554-575.
3. Budden, K.G., *Report of the Physical Society Conference on the Physics of the Ionosphere*, Cavendish Laboratory, Cambridge, (1955), 332.
4. Wright, J.W. and Norton, R.B., N. B.S. Tech Note #14, 1959.
5. Haselgrove, J., *The Physics of the Ionosphere*, Sept. 1954, 355.
6. Cooper, W.W., RADC-TM-61-1.

GLOSSARY OF TERMS

μ	- refractive index
r, θ, ϕ	- earth-centered co-ordinates of the ray path
$\rho_r, \rho_\theta, \rho_\phi$	- components of a vector of length μ, directed normal to the phase fronts (called the wave normal vector)
t	- time of phase travel along the path
h	- magnitude of earth's magnetic field
h_r, h_θ, h_ϕ	- components of magnetic field in the r, θ, ϕ directions
N	- number of electrons per cubic meter
F	- frequency of transmission (from 10 to 30 MC)
a	- $\frac{81N}{F^2}$
F_h	- gyro frequency of earth (constant at 1.3 MC)
α	- angle between wave normal vector and the earth's magnetic field vector
x	- height above the earth's surface divided by the radius of the earth
R_0	- radius of the earth (6380 KM)
i_0	- elevation angle at which the ray is initially sent out
l	- azimuthal angle at which the ray is initially sent out
T	- group time
G	- $\left(\frac{F_h}{F}\right)^2$

CATALOGUE FILE CARD

Rome Air Development Center, Griffiss AF Base, N.Y. Rpt No. RADC-TDR-62-473. H-F PROPAGATION SIMULATION. November 1962, 21p. incl illus.
Unclassified Report

An experiment is described in which high frequency electromagnetic wave propagation is to be simulated on an analog computer and compared with experimental data collected over a 3800-KM path. The experimental complex consists of a transmitter site located in the Panama Canal Zone and a receiver site at Stockbridge, N.Y. Vertical ionospheric sounders are located along the transmission path and are used to measure the spatial distribution of electron density in the volume of interest. A method is described whereby this spatial distribution of electron density is programmed into the analog computer in order that the Hamiltonian equations describing ray paths may be solved. In addition to producing frequency vs. time plots for comparison with the experimental data, the simulator also gives results not easily measured in

1. Electromagnetic Waves
2. Simulation
I. R. Mather, F. Wilson
II. In ASTIA collection

Rome Air Development Center, Griffiss AF Base, N.Y. Rpt No. RADC-TDR-62-473. H-F PROPAGATION SIMULATION. November 1962, 21p. incl illus.
Unclassified Report

An experiment is described in which high frequency electromagnetic wave propagation is to be simulated on an analog computer and compared with experimental data collected over a 3800-KM path. The experimental complex consists of a transmitter site located in the Panama Canal Zone and a receiver site at Stockbridge, N.Y. Vertical ionospheric sounders are located along the transmission path and are used to measure the spatial distribution of electron density in the volume of interest. A method is described whereby this spatial distribution of electron density is programmed into the analog computer in order that the Hamiltonian equations describing ray paths may be solved. In addition to producing frequency vs. time plots for comparison with the experimental data, the simulator also gives results not easily measured in

1. Electromagnetic Waves
2. Simulation
I. R. Mather, F. Wilson
II. In ASTIA collection

Rome Air Development Center, Griffiss AF Base, N.Y. Rpt No. RADC-TDR-62-473. H-F PROPAGATION SIMULATION. November 1962, 21p. incl illus.
Unclassified Report

An experiment is described in which high frequency electromagnetic wave propagation is to be simulated on an analog computer and compared with experimental data collected over a 3800-KM path. The experimental complex consists of a transmitter site located in the Panama Canal Zone and a receiver site at Stockbridge, N.Y. Vertical ionospheric sounders are located along the transmission path and are used to measure the spatial distribution of electron density in the volume of interest. A method is described whereby this spatial distribution of electron density is programmed into the analog computer in order that the Hamiltonian equations describing ray paths may be solved. In addition to producing frequency vs. time plots for comparison with the experimental data, the simulator also gives results not easily measured in

1. Electromagnetic Waves
2. Simulation
I. R. Mather, F. Wilson
II. In ASTIA collection

Rome Air Development Center, Griffiss AF Base, N.Y. Rpt No. RADC-TDR-62-473. H-F PROPAGATION SIMULATION. November 1962, 21p. incl illus.
Unclassified Report

An experiment is described in which high frequency electromagnetic wave propagation is to be simulated on an analog computer and compared with experimental data collected over a 3800-KM path. The experimental complex consists of a transmitter site located in the Panama Canal Zone and a receiver site at Stockbridge, N.Y. Vertical ionospheric sounders are located along the transmission path and are used to measure the spatial distribution of electron density in the volume of interest. A method is described whereby this spatial distribution of electron density is programmed into the analog computer in order that the Hamiltonian equations describing ray paths may be solved. In addition to producing frequency vs. time plots for comparison with the experimental data, the simulator also gives results not easily measured in

1. Electromagnetic Waves
2. Simulation
I. R. Mather, F. Wilson
II. In ASTIA collection

CATALOGUE FILE CARD

the field, such as take-off angle, angle of arrival, group time, phase time, off-path deviation, and height of reflection. An alternate use for the simulator is also presented. By rescaling the problem and making use of its capability to generate functions of three variables, one can examine the effects of small-scale irregularities of ionization on electromagnetic waves.		the field, such as take-off angle, angle of arrival, group time, phase time, off-path deviation, and height of reflection. An alternate use for the simulator is also presented. By rescaling the problem and making use of its capability to generate functions of three variables, one can examine the effects of small-scale irregularities of ionization on electromagnetic waves.	
the field, such as take-off angle, angle of arrival, group time, phase time, off-path deviation, and height of reflection. An alternate use for the simulator is also presented. By rescaling the problem and making use of its capability to generate functions of three variables, one can examine the effects of small-scale irregularities of ionization on electromagnetic waves.		the field, such as take-off angle, angle of arrival, group time, phase time, off-path deviation, and height of reflection. An alternate use for the simulator is also presented. By rescaling the problem and making use of its capability to generate functions of three variables, one can examine the effects of small-scale irregularities of ionization on electromagnetic waves.	

CATALOGUE FILE CARD

Rome Air Development Center, Griffiss AF Base, N.Y.
Rpt No. RADC-TDR-62-473. H-F PROPAGATION SIMULATION. November 1962, 21p. incl illus.
Unclassified Report

An experiment is described in which high frequency electromagnetic wave propagation is to be simulated on an analog computer and compared with experimental data collected over a 3800-KM path. The experimental complex consists of a transmitter site located in the Panama Canal Zone and a receiver site at Stockbridge, N.Y. Vertical ionospheric sounders are located along the transmission path and are used to measure the spatial distribution of electron density in the volume of interest. A method is described whereby this spatial distribution of electron density is programmed into the analog computer in order that the Hamiltonian equations describing ray paths may be solved. In addition to producing frequency vs. time plots for comparison with the experimental data, the simulator also gives results not easily measured in

1. Electromagnetic Waves
2. Simulation
I. R. Mather, F. Wilson
II. In ASTIA collection

Rome Air Development Center, Griffiss AF Base, N.Y.
Rpt No. RADC-TDR-62-473. H-F PROPAGATION SIMULATION. November 1962, 21p. incl illus.
Unclassified Report

An experiment is described in which high frequency electromagnetic wave propagation is to be simulated on an analog computer and compared with experimental data collected over a 3800-KM path. The experimental complex consists of a transmitter site located in the Panama Canal Zone and a receiver site at Stockbridge, N.Y. Vertical ionospheric sounders are located along the transmission path and are used to measure the spatial distribution of electron density in the volume of interest. A method is described whereby this spatial distribution of electron density is programmed into the analog computer in order that the Hamiltonian equations describing ray paths may be solved. In addition to producing frequency vs. time plots for comparison with the experimental data, the simulator also gives results not easily measured in

1. Electromagnetic Waves
2. Simulation
I. R. Mather, F. Wilson
II. In ASTIA collection

Rome Air Development Center, Griffiss AF Base, N.Y.
Rpt No. RADC-TDR-62-473. H-F PROPAGATION SIMULATION. November 1962, 21p. incl illus.
Unclassified Report

An experiment is described in which high frequency electromagnetic wave propagation is to be simulated on an analog computer and compared with experimental data collected over a 3800-KM path. The experimental complex consists of a transmitter site located in the Panama Canal Zone and a receiver site at Stockbridge, N.Y. Vertical ionospheric sounders are located along the transmission path and are used to measure the spatial distribution of electron density in the volume of interest. A method is described whereby this spatial distribution of electron density is programmed into the analog computer in order that the Hamiltonian equations describing ray paths may be solved. In addition to producing frequency vs. time plots for comparison with the experimental data, the simulator also gives results not easily measured in

1. Electromagnetic Waves
2. Simulation
I. R. Mather, F. Wilson
II. In ASTIA collection

Rome Air Development Center, Griffiss AF Base, N.Y.
Rpt No. RADC-TDR-62-473. H-F PROPAGATION SIMULATION. November 1962, 21p. incl illus.
Unclassified Report

An experiment is described in which high frequency electromagnetic wave propagation is to be simulated on an analog computer and compared with experimental data collected over a 3800-KM path. The experimental complex consists of a transmitter site located in the Panama Canal Zone and a receiver site at Stockbridge, N.Y. Vertical ionospheric sounders are located along the transmission path and are used to measure the spatial distribution of electron density in the volume of interest. A method is described whereby this spatial distribution of electron density is programmed into the analog computer in order that the Hamiltonian equations describing ray paths may be solved. In addition to producing frequency vs. time plots for comparison with the experimental data, the simulator also gives results not easily measured in

1. Electromagnetic Waves
2. Simulation
I. R. Mather, F. Wilson
II. In ASTIA collection

CATALOGUE FILE CARD

the field, such as take-off angle, angle of arrival, group time, phase time, off-path deviation, and height of reflection. An alternate use for the simulator is also presented. By rescaling the problem and making use of its capability to generate functions of three variables, one can examine the effects of small-scale irregularities of ionization on electromagnetic waves.		the field, such as take-off angle, angle of arrival, group time, phase time, off-path deviation, and height of reflection. An alternate use for the simulator is also presented. By rescaling the problem and making use of its capability to generate functions of three variables, one can examine the effects of small-scale irregularities of ionization on electromagnetic waves.	
the field, such as take-off angle, angle of arrival, group time, phase time, off-path deviation, and height of reflection. An alternate use for the simulator is also presented. By rescaling the problem and making use of its capability to generate functions of three variables, one can examine the effects of small-scale irregularities of ionization on electromagnetic waves.		the field, such as take-off angle, angle of arrival, group time, phase time, off-path deviation, and height of reflection. An alternate use for the simulator is also presented. By rescaling the problem and making use of its capability to generate functions of three variables, one can examine the effects of small-scale irregularities of ionization on electromagnetic waves.	

UNCLASSIFIED